REPORT OF THE SPATIAL ANALYSIS OF PART OF FORT BENNING USING REMOTE IMAGERY

Final Report (RSSUSA - 4)

Dr Margaret A. Oliver and Professor Richard Webster

August 1995 to November 1995

United States Army

ENVIRONMENTAL RESEARCH OFFICE OF THE U.S. ARMY

London, England

CONTRACT NUMBER - N68171 - 95 - C - 9007

DISCLAIMER NOTICE

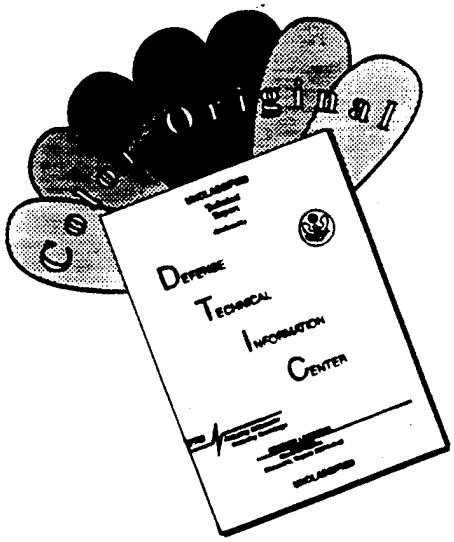

THIS DOCUMENT IS BEST QUALITY AVAILABLE. THE COPY FURNISHED TO DTIC CONTAINED A SIGNIFICANT NUMBER OF COLOR PAGES WHICH DO NOT REPRODUCE LEGIBLY ON BLACK AND WHITE MICROFICHE.

REPORT OF THE SPATIAL ANALYSIS OF PART OF FORT BENNING USING REMOTE IMAGERY

Final Report (RSSUSA - 4)

Dr Margaret A. Oliver and Professor Richard Webster

August 1995 to November 1995

United States Army

ENVIRONMENTAL RESEARCH OFFICE OF THE U.S. ARMY

London, England

CONTRACT NUMBER - N68171 - 95 - C - 9007

REPORT DOCUMENTATION PAGE

Form Approved
OMB No. 0704-0188

1. AGENCY USE ONLY (Leave blank)	2. REPORT DATE	3. REPORT TYPE AND DATES COVERED

4. TITLE AND SUBTITLE
Final Report on Phase 1 of Optimizing Field Sample Design from Remote Imagery

5. FUNDING NUMBERS
PR-N 68171
95-C-9007

6. AUTHOR(S)
Dr M A Oliver, Professor R Webster

7. PERFORMING ORGANIZATION NAME(S) AND ADDRESS(ES)
University of Reading, Whiteknights, Reading, RG6 6DW

8. PERFORMING ORGANIZATION REPORT NUMBER
RSS USA-4

9. SPONSORING/MONITORING AGENCY NAME(S) AND ADDRESS(ES)
USARDGSG-UK
Environmental Sciences Branch,
Edison House, 233 Old Marylebone Road
London, NW1 5TH, UK

10. SPONSORING/MONITORING AGENCY REPORT NUMBER

11. SUPPLEMENTARY NOTES
Final Report

12a. DISTRIBUTION/AVAILABILITY STATEMENT
No limitations on distribution/availability

12b. DISTRIBUTION CODE

13. ABSTRACT (Maximum 200 words)

This final report summarises the three earlier ones and a detailed description of the second major analysis. The earlier reports included a literature review, a description of Fort Benning, and the exploratory data and variogram analyses of the spectral information from the study area (a small part of the Fort). The results showed that channels 2 and 3 are highly correlated, but neither is with channel 1. The variograms for the rows and columns of the spectral data and their averages for all three channels and NDVI (normalized difference vegetation index) show the same spatial structure. There are two spatial scales, the short one is 9 pixels (180 m) and the long one 144 pixels (2880 m). A transect sampling was designed for reconnaissance based on the short range variation to determine ground cover. The analysis of these data showed that the structure in the variation of the image reflected that in the ground cover closely. A second sampling scheme based on a nested grid with intervals of 1500 m and 75 m was designed for fieldwork. Our major conclusion at this stage is that it appears reasonable to design a sampling scheme for fieldwork directly from the image in the data without the need for the reconnaissance stage.

14. SUBJECT TERMS	15. NUMBER OF PAGES
Geostatistics, Grid, Modelling, Sampling, Spatial Scale, Transects, Variogram, Vegetation.	16. PRICE CODE

17. SECURITY CLASSIFICATION OF REPORT	18. SECURITY CLASSIFICATION OF THIS PAGE	19. SECURITY CLASSIFICATION OF ABSTRACT	20. LIMITATION OF ABSTRACT

NSN 7540-01-280-5500

Standard Form 298 (Rev. 2-89)
Prescribed by ANSI Std. Z39-18
298-102

ATTACHMENT 1
PAGE 1 OF 2

TABLE OF CONTENTS

ABSTRACT

This is the final report of the project with the US Army and TEC and contains a summary of the previous reports together with the results of the latest analyses. The main aims of this work have been to determine the structure in the reflectance information for a Region of interest in a SPOT image covering Fort Benning. Based on the information from a variogram analysis of the three wavebands and the normalized difference vegetation index (NDVI) an optimal sampling scheme using ten transects was designed to examine the ground cover. There were two distinct scales of spatial variation, one with a short range of 180 m (9 pixels) and the other with a range of about 3 km (150 pixels). The shorter of these was chosen to examine the ground cover. The structure of the variation in the latter matched that of the reflectance closely, suggesting that the image represents changes in ground cover reliably.

Finally an optimal sampling scheme for field survey was designed using the ground cover information from the transect survey in conjunction with the raw data from the image. This was less intense than we wanted; it was based on the resources available for fieldwork at the time. Ultimately the aim is to use remote imagery of the same kind to aid routine survey of ground cover and management decisions.

INTRODUCTION

The United States Army's training grounds are also the habitats of endangered species. The Army is now concerned with protecting the environment of these sites, and it wishes to restore them as far as possible while still using them. To these ends it needs to know the extent of such habitats and of current damage, and then to monitor change, deterioration or improvement, both locally and regionally. This requires mapping.

The project is part of a wider brief. The help of the US Army's Topographic Engineering Center (TEC) has been enlisted to introduce new technology for assessing and monitoring the condition of such sites and to advise on the rehabilitation of the training grounds so that vegetation will regenerate and the habitats of certain protected species will re-establish. TEC has enlisted our help to apply geostatistical methods of spatial analysis to the problem. This particular project will assess the sampling interval needed to resolve the spatial variation in the ground cover.

The main aims of this project have been to design optimal sampling schemes from the reflectance information of a SPOT x 3 image and to examine the ground cover so that any spatial structures present in both can be compared, and for mapping. The assumption underlying the idea is that the pattern in the image relates to meaningful information on the ground. As a first requirement the spatial scales in the image must be the same as those of the features on the ground, e.g. the vegetation or the landform. The SPOT image covered Fort Benning, and an area of 5 km $\times$ 5 km within it was chosen for the detailed analysis. The latter was the study area, and it

is called the Region in the rest of the report.

The information gained from the analysis, in particular the variogram analysis, has enabled us to evaluate the information in the image as a basis for designing sampling schemes directly from the information in the image. If this is feasible it could save effort. Resources for survey are inevitably limited, and so there is a need to obtain as much information as possible with the available resources or to find the resources needed to produce an adequate solution.

This report contains a summary of the three earlier interim reports together with the most recent results. It describes the study area, the data from the SPOT image, the analysis and results in detail.

SPOT IMAGE AND STUDY AREA

The SPOT image of Columbus, Georgia, which includes all of Fort Benning was recorded in November 1994. Fort Benning covers some 70% of the area of the image. The pixels of the image have a resolution on the ground of about 20 m $\times$ 20 m. There are three wave bands namely: Green, Red and Near Infra Red (NIR) in that order. The terrain is heavily dissected and wooded with many species of tree. The plant communities are heterogeneous.

Fort Benning is a heavy artillery training installation operating under US Army Forces Command. As the frequency and intensity of training has increased so has the damage to the soil surface and vegetation. The demands of training conflict with those of protecting the environment. Specifically, soil erosion is severe wherever the land has been cleared (at McKenna Hill for instance). Kudzu is spreading uncontrollably and choking other vegetation, and the habitat of several endangered species such as the Red Cockaded Woodpecker (RCW), is threatened. The Integrated Training Area Management (ITAM) programme aims to balance the training needs with those of the environment by attempting to maintain the sites in as natural a condition as possible.

EXISTING INFORMATION

Much information has already been collected on the vegetation of the Fort as part of the ITAMS inventory. There is some concern as to how representative this information is and whether the basis of recording is the best possible. For instance, is the sampling interval adequate to resolve the spatial variation in the ground cover at the chosen scale of investigation? This project examines an optimal scheme for obtaining representative information, i.e. for obtaining the required information with minimal field work. However, we could not be certain that this would be an improvement on the ITAMS (Land Condition-Trend Analysis) information.

PROGRAMME OF WORK

At the outset we reviewed the substantial pertinent literature. We chose the book

by Richards (1993) on remote sensing as a handbook. It covers all the essential topics and is up to date. We have also familiarized ourselves with the facilities offered by IMAGINE (Langford, 1983) – this is the main digital image processing package used, and it is available at the University of Reading. The other relevant papers and books for this project are listed in the Bibliography.

The following is a summary of the more important papers. Van Der Meer (1993) used geostatistics, in particular indicator kriging, to classify spectral information directly without any prior knowledge from the training data. He showed that it performed better than conventional classification methods. This is important in terms of how the sampling should be optimized. Bonifazi *et al.* (1993) used a neural net approach to discriminate between different urban areas on an image. Goossens *et al.* (1993) applied spatial filtering techniques in classifiying remotely sensed data. They also discussed the problem of loss of information with classification, and how the reliability of classification depended on the relations between pixels in a given neighbourhood, i.e. the degree and extent of spatial dependence. The latter is also crucial in deciding how to sample.

Vairinho *et al.* (1993) used kriging in combination with image processing methods and found that this enhanced specific features of the image to obtain the best classification. Atkinson *et al.* (1990) showed how economy can be achieved by sampling remotely sensed data. Spatial dependence and strong correlation in the wavebands mean that the data contain much redundant information, and so it is important to improve efficiency. The sampling scheme chosen for the purpose will depend on what is known already of the spatial variation, and its results will also help future understanding and further improvements in sampling. Atkinson *et al.* (1990) tested optimal sampling of images and reconstruction based on kriging using data from an airborne scanner at 600 m. They have since shown how to plan the combination of ground sampling and radiometric data in different wavebands to optimize the use of resources (Atkinson *et al.*, 1992, 1994). The geostatistical approach to sampling has been explored to some extent to identify objects in imagery Woodcock *et al.* (1988 a and b).

Once we had the SPOT data for the Region we determined the spatial scale and structure of the variation in them using the variogram. All three wave bands and the normalized difference vegetation index (NDVI) were examined. The last is a standard measure to represent vegetation (see page 5). The variograms were modelled mathematically, and based on the parameters of these models we designed an optimal sampling scheme for the first period of fieldwork in July 1995 based on ten transects located in a stratified random way. TEC decided that it was the shorter of the two ranges of variation that emerged from the variogram analysis that was of interest hence the transect sampling scheme proposed has focused on this. The aim was to examine the dominant ground cover in a predefined way for each sampling area, which should correspond with the pixel in the image.

When we had established that the scale of variation in the spectral information

corresponded closely with that of the ground cover we designed a sampling scheme for mapping. At this stage the aims of the project had to be modified because of the difficulties of obtaining adequate data in the time available for sampling. Over 2000 field samples would have been required to ensure that the vegetation data were spatially dependent for interpolation. A nested grid was used that took into account the two main scales of spatial variation. Based on the results of the first sampling it should be possible to design sampling schemes directly from the information in the image in future.

ANALYSIS AND RESULTS

We started with an exploratory data analysis of the spectral information in the image of Fort Benning which determined the means, variances, and the departure from normality. We then analysed these data geostatistcally. The purpose of the variogram analysis was to describe the spatial structure in the Region from the SPOT image so that a reconnaissance sampling scheme for a field survey could be designed. The results provided a basis for the sampling scheme to obtain field data to correlate with the image. A sampling scheme using transects was chosen for determining the ground cover in the field, and to relate this to the pixel information in the wavebands. Ground information had therefore to be obtained from quadrats that matched the SPOT pixels in both position and size, i.e. 20 m $\times$ 20 m. It was decided to record the cover of each pixel as a single class representing the dominant species.

The pixel maps of the three wave bands are shown in Figures 1 to 3. An attempt was made to show approximately the same amount of detail in the variation in each of the wavebands, hence the scales of the reflectance values are different. The normalized difference vegetation index, NDVI (D), was computed from bands 2 (Red) and 3 (Infra-red) by

$$D = (I - R)/(I + R) ,$$

where I and R are the values in the near infra-red and red channels respectively. The NDVI is also shown as a map, Figure 4.

The statistical distributions of the three wavebands and NDVI were determined and are given in Table 1. The data in channel 1 was approximately symmetrical, but those in channels 2 and 3 were strongly positively skewed, and we transformed them to stabilize their variances for further analysis. The transformation was

$$z_t = \log_{10}(z - b) ,$$

where b is a shift, 22 for channel 2 and 37 for channel 3.

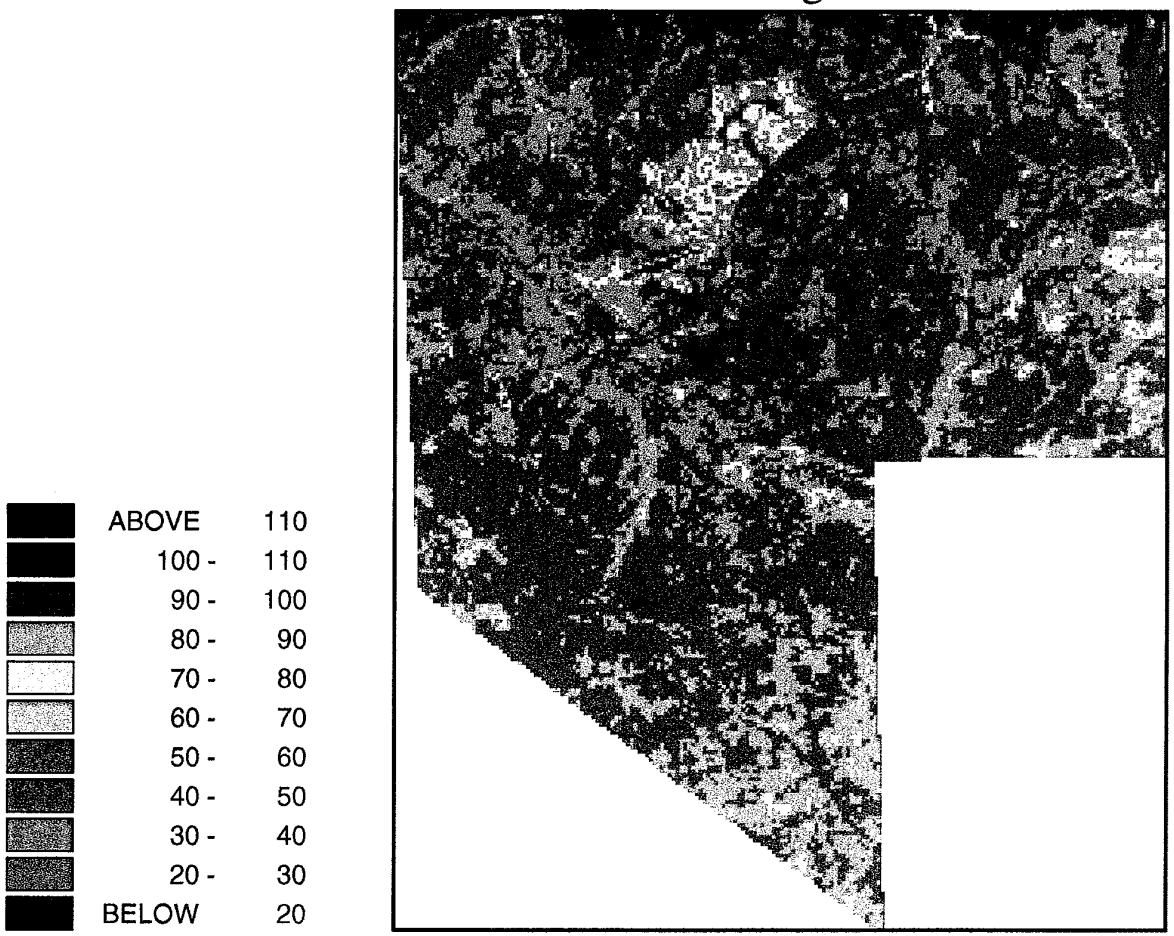

Figure 1. Pixel map of spectral values for channel 1

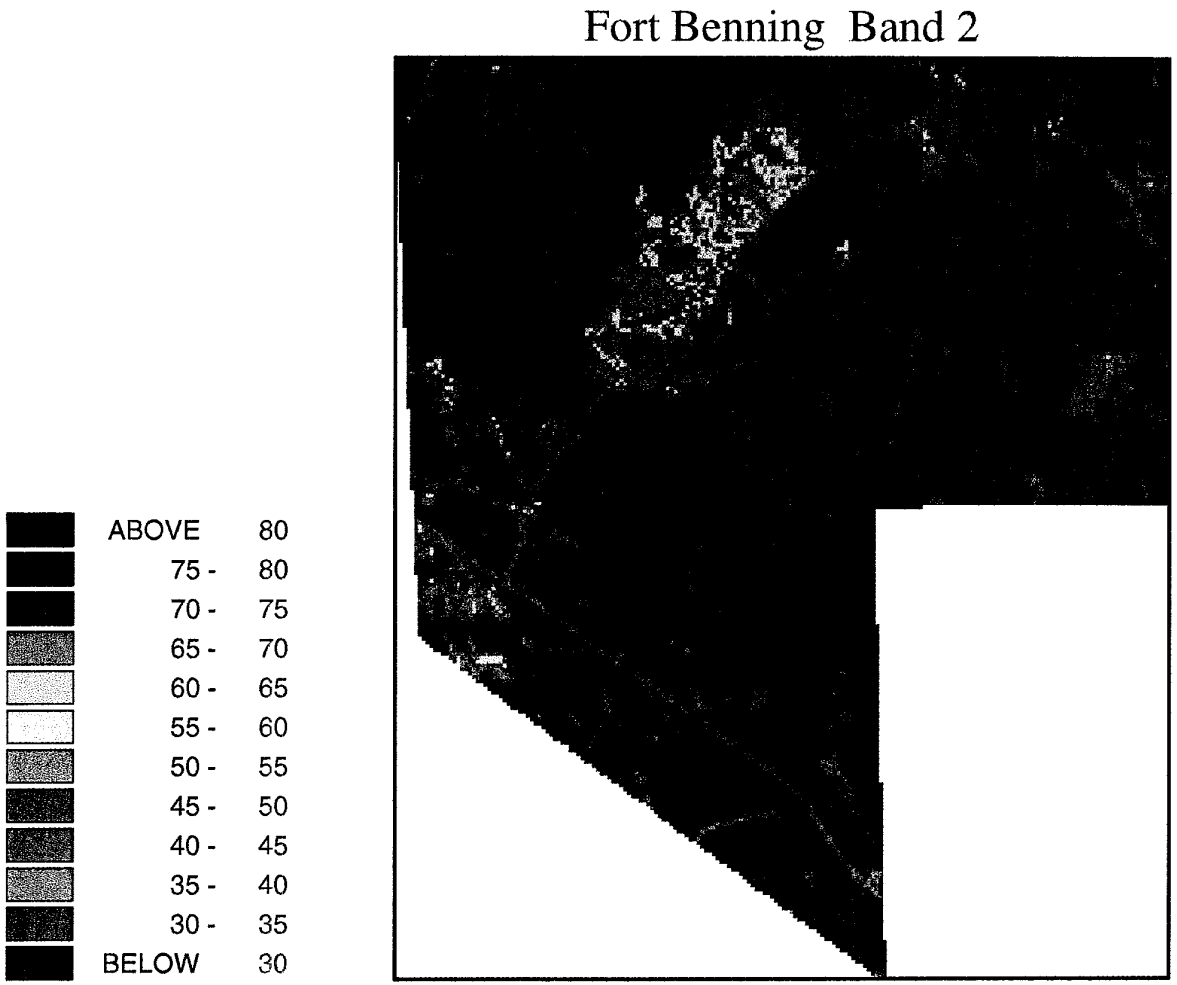

Figure 2. Pixel map of spectral values for channel 2

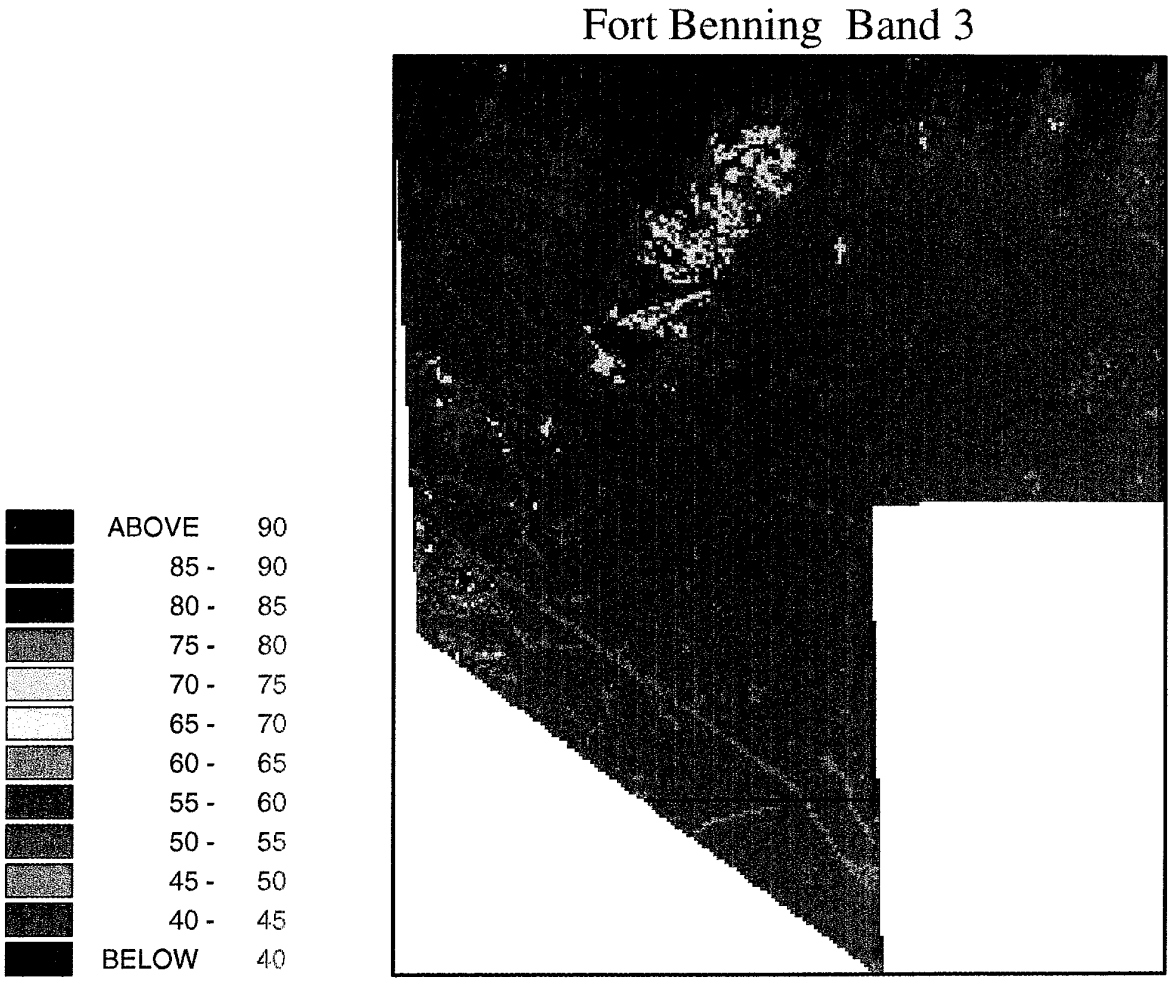

Figure 3. Pixel map of spectral values for channel 3

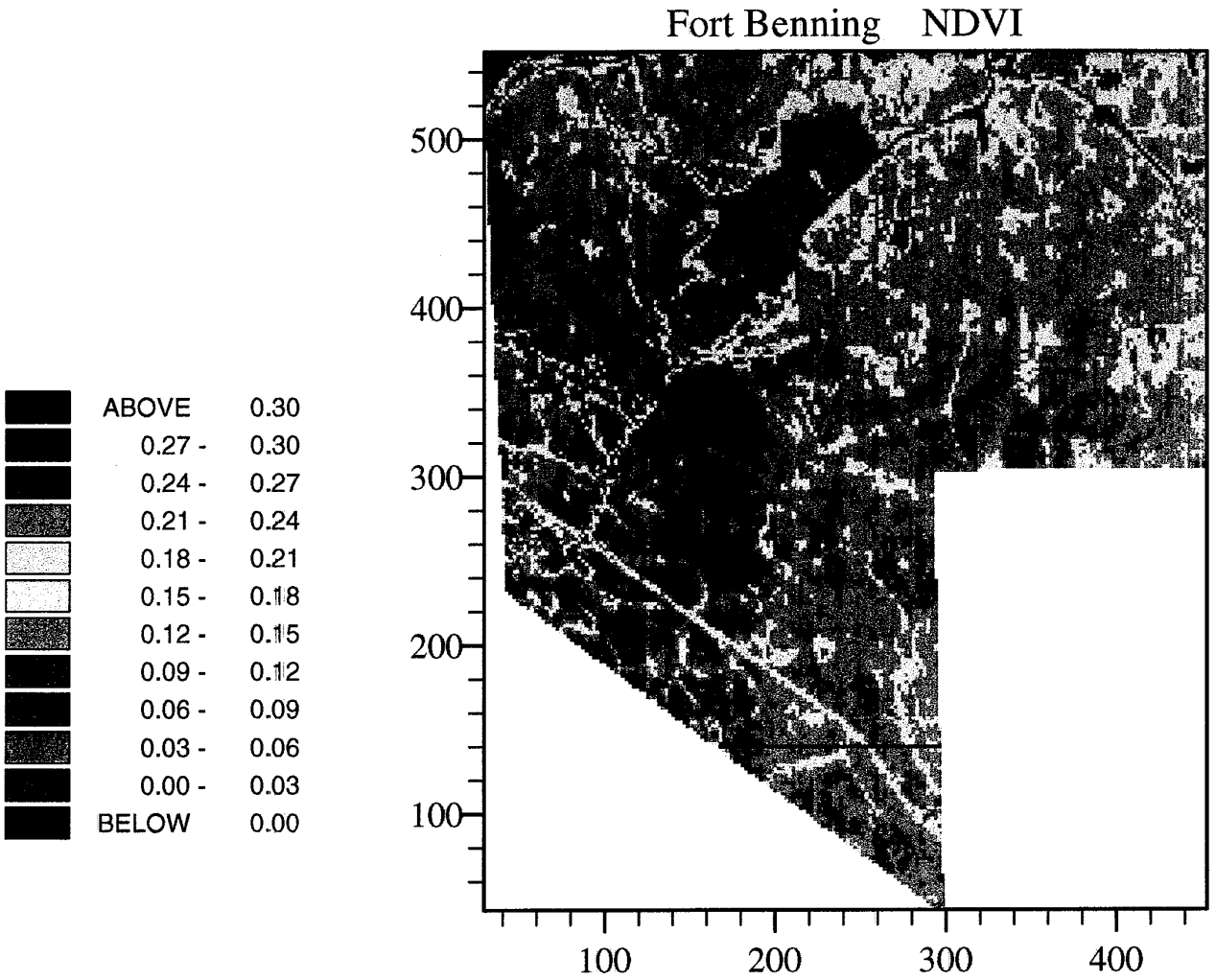

Figure 4. Pixel map of spectral values for NDVI

Table 1. Summary Statistics

Channel	Minimum	Maximum	Mean	Variance	St. Dev.	Skewness
1	17.0	125.0	58.5	69.84	8.35	0.66
2 original	23.0	128.0	29.4	92.33	9.61	4.18
2 $\log_{10}(x-22)$	0	2.025	0.721	0.09317	0.305	1.47
3 original	38.0	137.0	44.0	38.46	6.20	4.41
3 $\log_{10}(x-37)$	0	2.000	0.802	0.04617	0.215	1.72
NDVI	−0.356	0.567	0.337	0.009672	0.098	−1.93

The correlation coefficients for the wavebands were computed. The information in channel 1 is moderately correlated with that in channels 2 and 3, but not so strongly as to represent serious redundancy. The data in channels 2 and 3, however, are strongly dependent.

Table 2. Correlation matrix of three channels

channel	1	2
2	0.663	
3	0.677	0.946

Variogram Analysis

Variograms were computed for the rows and columns separately and also as averages of the rows and columns using the usual computing formula:

$$\widehat{\gamma}(\mathbf{h}) \quad = \quad \frac{1}{2m(\mathbf{h})} \sum_{i=1}^{m(\mathbf{h})} \{z(\mathbf{x}_i) - z(\mathbf{x}_i + \mathbf{h})\}^2 \ .$$

where $\widehat{\gamma}(\mathbf{h})$ is the estimate of $\gamma(\mathbf{h})$ (the semivariance) at lag $\mathbf{h}$, $z(\mathbf{x}_i)$ and $z(\mathbf{x}_i + \mathbf{h})$ are the observed values of Z in any one waveband at $\mathbf{x}_i$ and $\mathbf{x}_i + \mathbf{h}$, respectively, and $m(\mathbf{h})$ is the number of paired comparisons at that lag. By changing $\mathbf{h}$ we obtained a set of semivariances, which is the *experimental variogram* or *sample variogram.*

For channels 2 and 3 the transformed values were used. Authorized models were then fitted to all the sets of experimental results using the program MLP (Ross, 1987).

Variogram Results

The experimental variograms for the three channels and NDVI for both rows and columns have a similar form—they all show strong evidence of spatial correlation, Figure 5. The best fitting model in every instance was the double exponential or nested exponential:

$$\gamma(h) \;=\; c_0 + c_1\{1 - \exp(-h/a_1)\} + c_2\{1 - \exp(h/a_2)\}\ ,$$

where c_0 is the nugget variance, c_1 and a_1 are the sill and distance parameter of a short-range component of variance, and c_2 and a_2 are the sill and distance parameter of a long-range component. The distance parameters a_1 and a_2 may be multiplied by 3 to give approximate correlation ranges for these components. Several other models, including power functions, spherical, double spherical, single exponential, pentaspherical, Whittle, and circular, were tried. None of these provided such a good fit as the double exponential model.

The fitted models suggest that there are two ranges of spatial variation, a short-range one averaging 9 pixels (180 m) and a long one of about 150 pixels (3 km), Table 3. The pattern in the variation of these wavebands and of NDVI occurs on two very distinct spatial scales. The variograms for NDVI have been recomputed since the previous report was prepared. The effective ranges for the NDVI are much the same as for the individual wave bands. The results are consistent, which suggests that they are reflecting a real pattern in the ground cover. The variograms of channels 2 and 3 are slightly different in that they show some divergence at lags greater than 25 pixels for channel 2 and at lags greater than 20 pixels for channel 3. The model parameters for the rows and columns are somewhat different, however, suggesting that there is some short-range anisotropy in the variation. The anisotropy is evident in the pixel maps, especially that for channel 1. In all cases the range of spatial dependence for the columns is greater, i.e., the patches that form the structures are elongated in the N–S direction. When the variograms were averaged over the rows and columns the same two ranges of spatial structure emerged (Figure 6). The graphs of the variograms for all of the above analyses look similar (Figures 5 and 6).

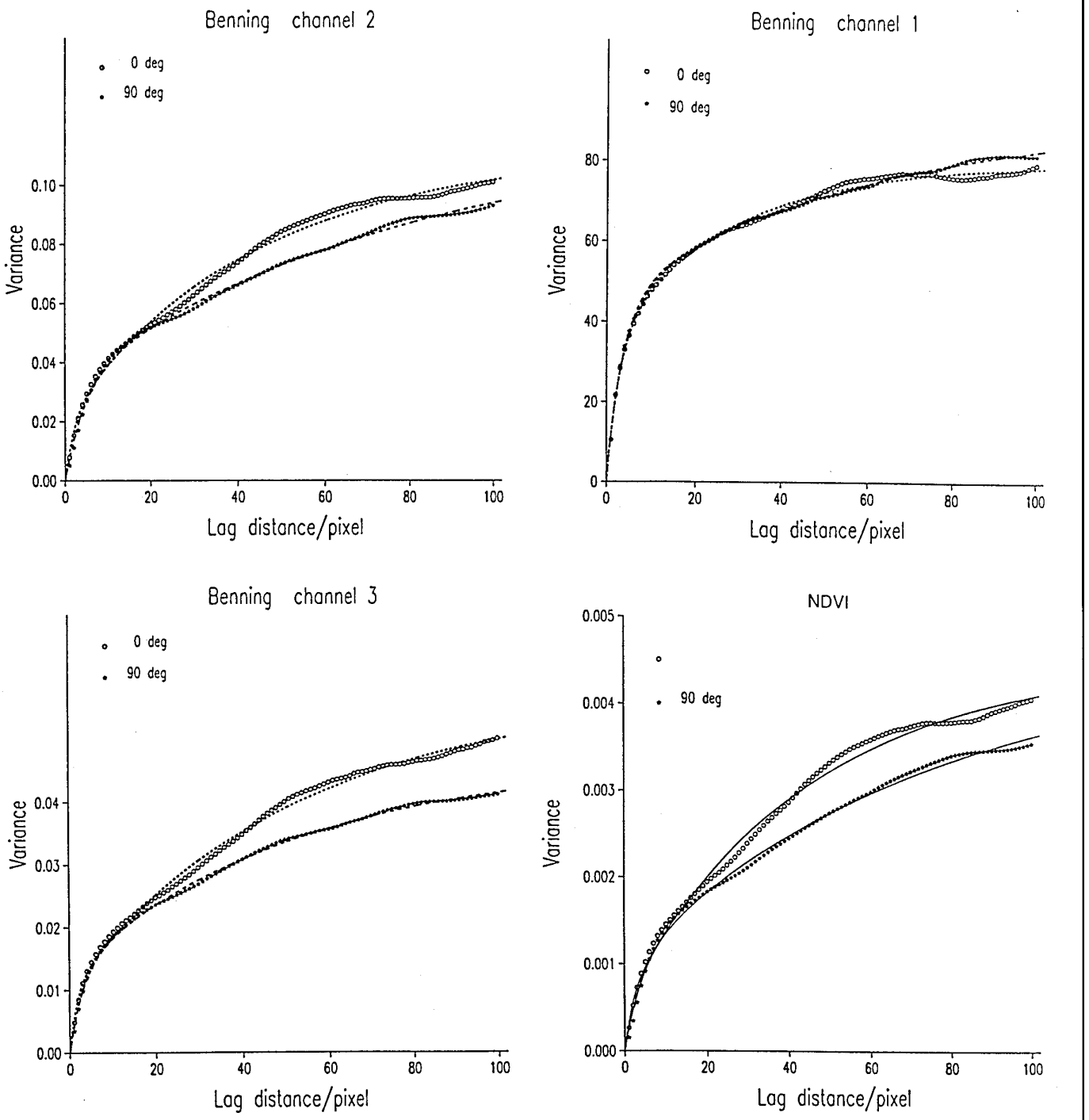

Figure 5. Variograms of rows and columns for channels 1, 2 and 3, and for NDVI. The symbols are the experimental semivariances, and the lines are the fitted models.

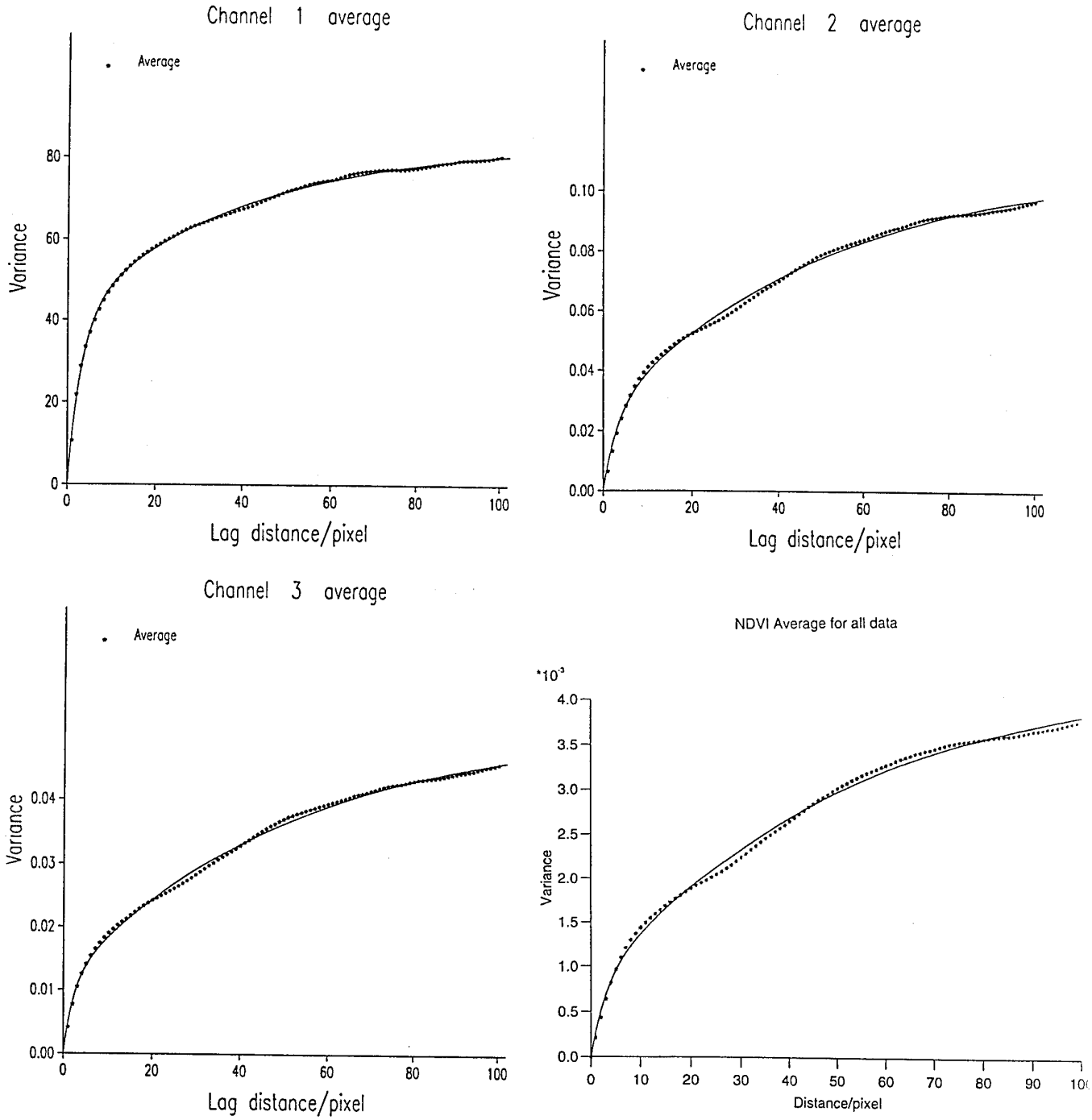

Figure 6. Average variograms for channels 1, 2 and 3, and NDVI. The symbols are the experimental semivariances, and the lines are the fitted models.

Table 3. Variogram model parameters for the three channels and NDVI

	Variance			Distance/pixels	
Channel	c_0	c_1	c_2	a_1	a_2
1 – rows	0	35.74	43.95	2.83	28.61
– columns	0.88	44.92	45.92	3.76	61.67
– average	0	40.84	42.71	3.26	38.87
2 – rows	0	0.0213	0.0904	2.19	44.67
– columns	0	0.0329	0.0854	4.49	79.00
– average	0	0.0262	0.0845	3.23	53.36
3 – rows	0	0.0105	0.0467	1.76	52.91
– columns	0	0.0130	0.0335	3.03	52.47
– average	0	0.0115	0.0400	2.33	51.92
NDVI					
– rows	0	0.00060	0.00393	1.90	45.40
– columns	0	0.00099	0.00359	4.16	74.60
– average	0	0.00076	0.00364	2.87	52.92

In the table c_0 is the nugget variance,
c_1 and c_2 are the sill variances of the short- and long-structures, respectively, and
a_1 and a_2 are the distance parameters of the short- and long-structures. For the exponential model these can be multiplied by 3 to obtain the effective ranges of spatial dependence.

The average effective range for the three bands was slightly less than 9 pixels, or 180 m, for the short-range variation, and 144 pixels, or 2880 m, for the long-range variation. These two spatial scales are an order of magnitude different, and this is likely to have important consequences for sampling.

FIRST SAMPLING

Based on the results of the variogram analysis and TEC's requirements we designed a sampling scheme to obtain ground data to match with that of the pixels in the image that would reflect the shorter range of variation. The two scales are so different that it was difficult to encompass both at this sampling stage where we wanted to obtain detailed information on the variation in ground cover. The aim was to determine to what extent the ground cover matches the pattern in the image, to relate them

quantitatively, and to model the coregionalization between the two. To achieve this the ground cover needs to have been recorded to match the pixels on the image exactly. Further, the pixels recorded in the field should be the same size and shape, i.e. be on the same support, as those in the image. The remote support is 20 m $\times$ 20 m for each pixel and so the field plots recorded must be the same. For each of the squares of this size its dominant cover, e.g. grass, bare ground, broad-leaved trees of kind x, coniferous trees of kind y, and so on were to have been determined and recorded as a single class. The data for each class would thus be of the presence-or-absence kind. Any one pixel would carry little information, and a satisfactory analysis would require data of this kind from more points than if variables were measured.

To interpret the short-range variation in the image we recommended sampling along transects. This is the best method at this stage to provide the data needed to determine the spatial structure in the ground cover, and to plan efficient sampling.

Transect Survey: Variogram Analysis

Ten transects, five in the E–W direction, i.e. along the rows of the image, and five in the N–S direction were chosen for recording ground cover in the field. Each transect was 100 pixels long to ensure that the short-range pattern was described in detail. The starting points for them were determined in a stratified random way which ensured that the ten transects were spread fairly evenly over the Region to represent it well. It was hoped that in the field contiguous plots (pixels), each 20 m $\times$ 20 m, corresponding to the pixels of the image, would be visited, and that the dominant cover of each would be recorded using a code. This scheme produced a sample of 1000 pixels, which although it might seem large was needed because the resulting data were qualitative, and so each item of information contributes little to the total. The need was to obtain records for many plots rather than detail within the plots to establish whether there was any correlation between the ground cover and the image information.

The transects did not enable the long-range component of the ground cover to be determined because this is, on average, more than 100 pixels long. If the long-range component had been chosen as the more important then we would have had two transects covering the full extent of one row and one column.

In the event it proved difficult to determine the cover on the ground. After attempting the fieldwork TEC discovered that with the resources available the only sensible way to obtain enough data to compute indicator variograms of the different kinds of cover was to use the aerial photographs for the site. So the dominant ground cover for each pixel was interpreted in this way.

Transect Survey: Variogram Results

There were 21 ground cover classes, but only those with more than 1.5% of the total cover were analysed fully, they were: long-leaf pine, 1, (13%), mixed pine, 3, (29%), loblolly pine, 4, (16%), short-leaf pine, 6, (1.5%), loblolly hard, 8, (12.5%),

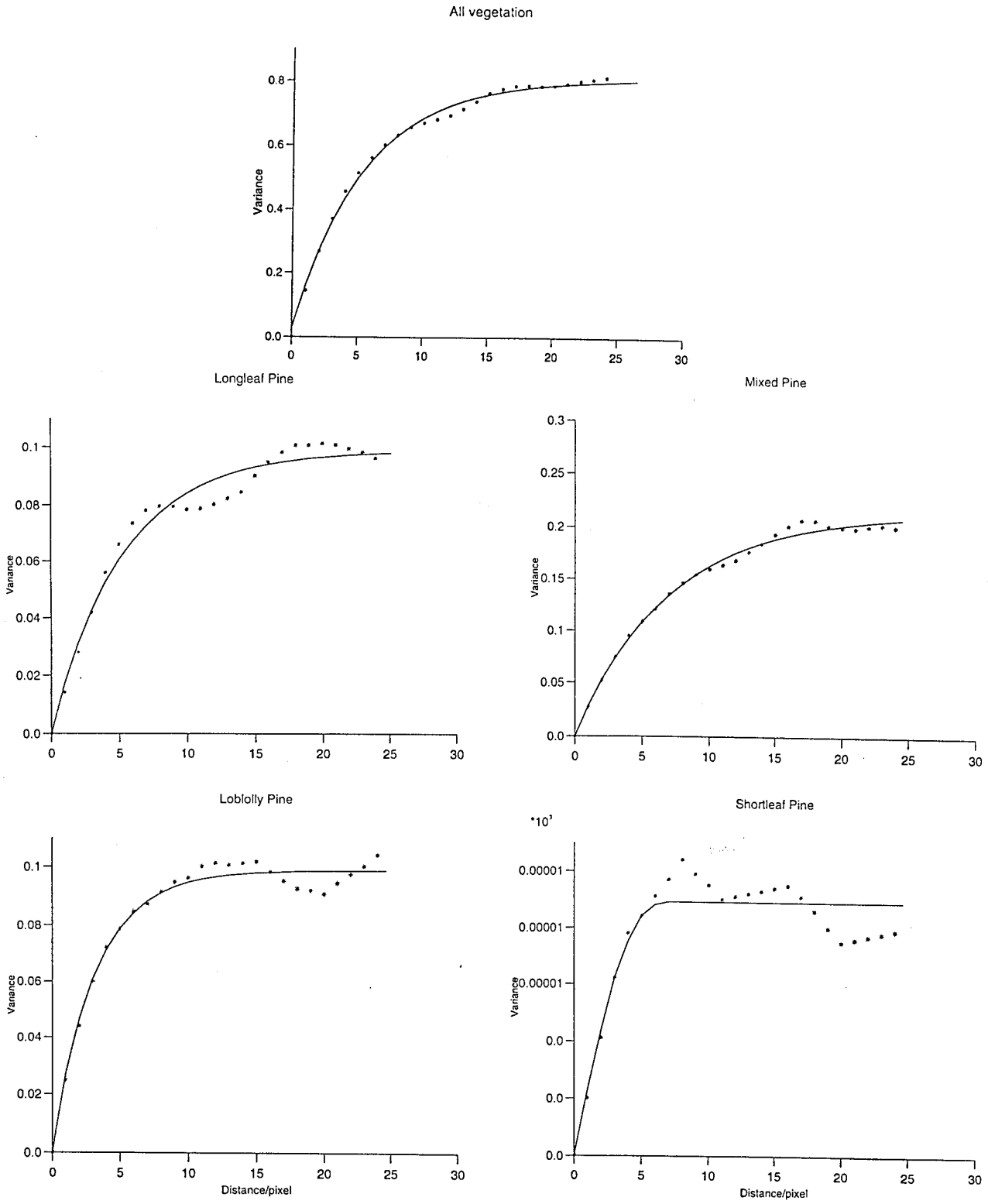

Figure 7. Experimental variograms of ground cover classes from the transect sampling.

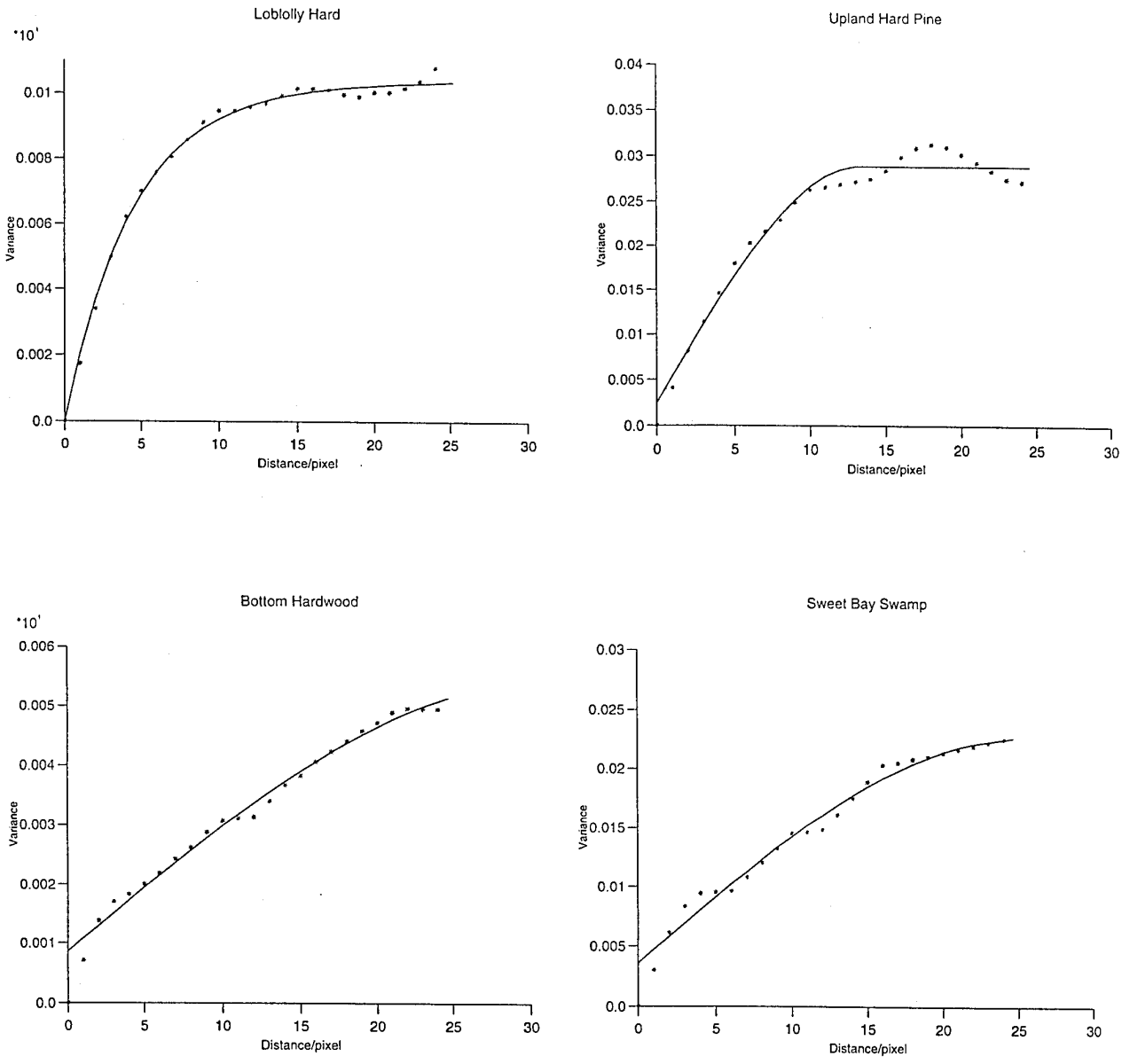

Figure 8. Experimental variograms of ground cover classes from the transect sampling.

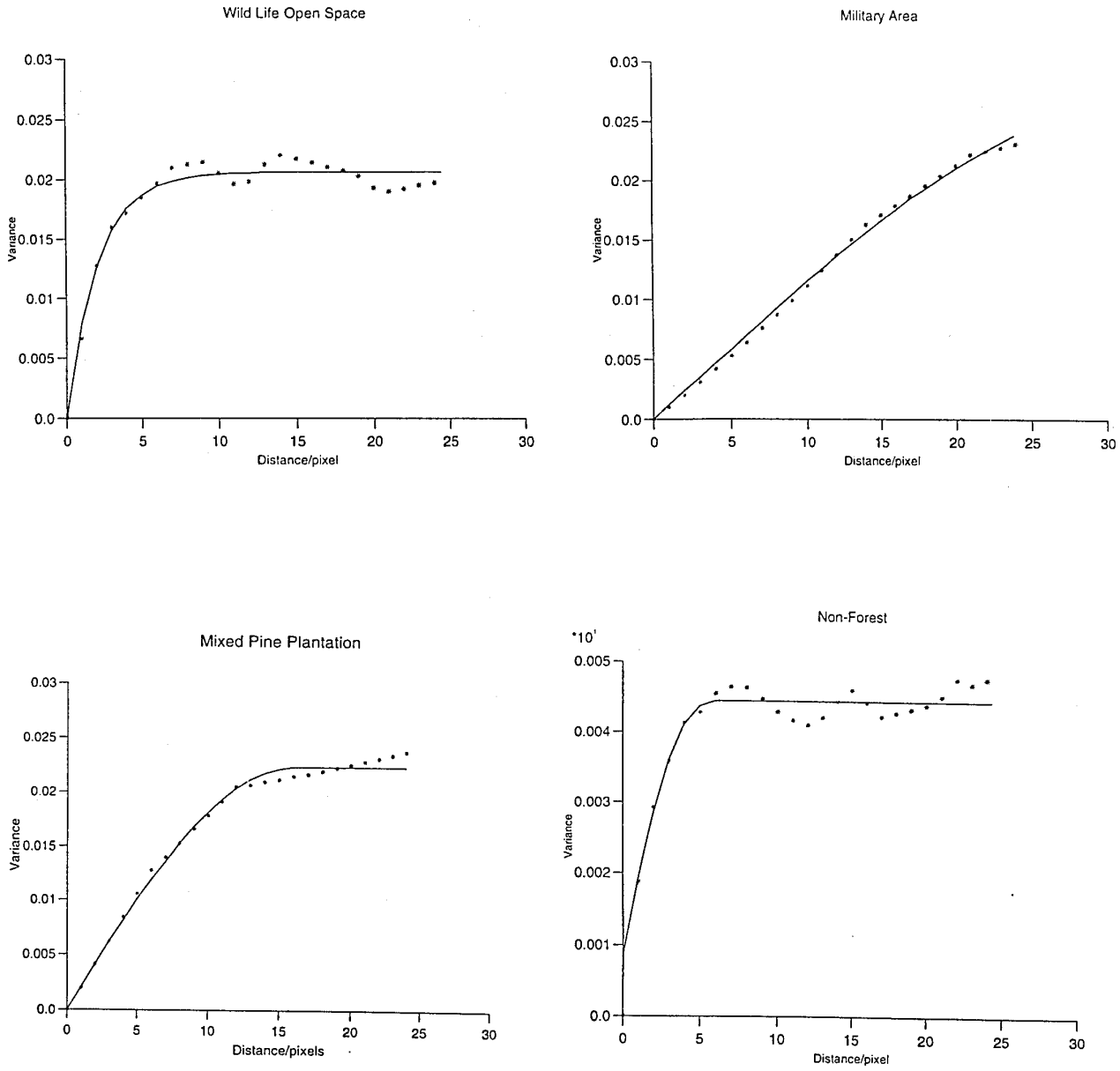

Figure 9. Experimental variograms of ground cover classes from the transect sampling.

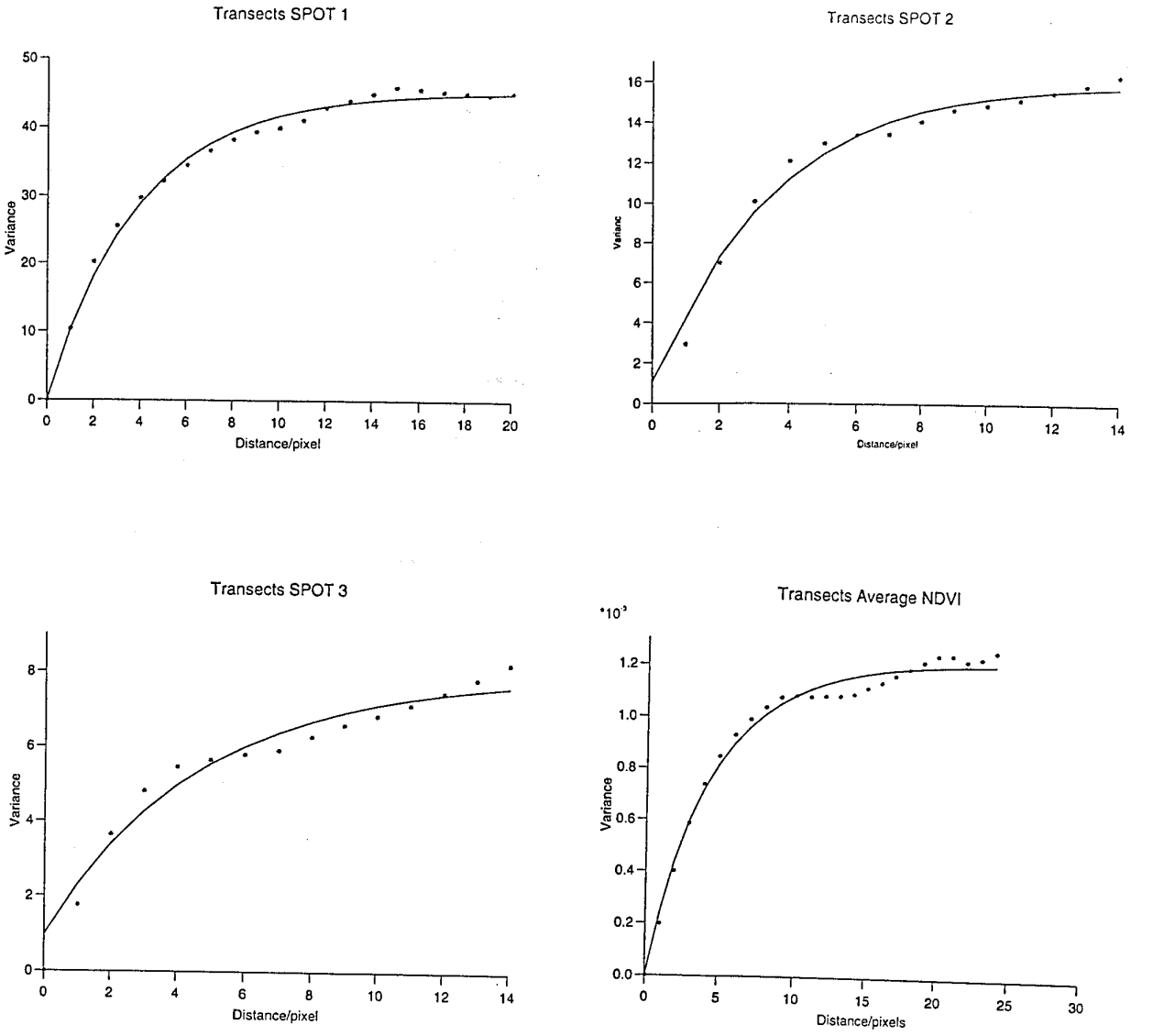

Figure 10. Variograms of Channels 1, 2 and 3, and NDVI for the transect data.

upland hard pine, 9, (3.25%), bottom hardwood, 11, (3.6%), sweet bay swamp, 20, (1.75%), wild life open space, 24, (2.5%), military, 30, (4.37%), mixed pine plantation, 33, (2.25%), non-forest, 34, (4.25%).

Experimental indicator variograms based on presence or absence were computed for each ground cover class, and for the sum of the indicators for all of the ground cover classes. The latter represents the likelihood of transition from one class to another. It is a good representation of the pattern in the ground cover classes. The model parameters are listed in Table 4 together with those for the data from the three wavebands for the transects and NDVI. The experimental variograms are shown in Figures 7 to 9. Half of the variograms were fitted best by an exponential model, including the variogram representing the average cover, Table 4. The other models were also bounded. The approximate ranges of the variograms fitted by exponential models are from 6 to 21 pixels (120 m to 420 m), with an average of 13 pixels (260 m). The average range of the variograms fitted by the other models is 16.5 pixels (330 m), and the variogram computed from the average of all the classes is 15 pixels (300 m). The results show that a consistent spatial structure is emerging for the ground cover with an approximate correlation range of 300 m.

Variograms were also computed for the spectral information in the three channels and for NDVI from the transect sample and modelled, Figure 10. Their model parameters are given in Table 4. These results for the transect data only mirrored the overall results. They were all fitted by an exponential model with approximate ranges of 13 pixels for channel 1, 10 pixels for channel 2, and 13 pixels for channel 3. This is also close to the average for the ground cover classes. Table 4 gives the parameters of these models.

Table 4. Model Parameters of Variograms for Cover Classes and SPOT Channels 1, 2 and 3. The models are defined below the Table.

	Variable	Model type	Parameters			
			r	a	c	c_0
	All cover types	Exponential	5.43		0.779	0.030
1	Long-leaf pine	Exponential	5.28		0.099	0
3	Mixed pine	Exponential	7.12		0.242	0
4	Loblolly pine	Exponential	3.15		0.099	0
6	Short-leaf pine	Pentaspherical		7.22	0.009	0
8	Loblolly hard	Exponential	4.56		0.104	0
9	Upland hard pine	Spherical		13.27	0.026	0.0024
11	Bottom hard wood	Spherical		30.97	0.045	0.0086
20	Sweet bay swamp	Spherical		25.39	0.0190	0.0036
24	Wild life open	Exponential	2.12		0.0207	0
30	Military	Spherical		35.31	0.0277	0
33	Mixed pine plantation	Spherical		16.16	0.0224	0
34	Non-forest	Pentaspherical		6.32	0.0357	0.0087
	SPOT 1	Exponential	4.42		42.44	3.45
	SPOT 2	Exponential	3.29		15.98	0
	SPOT 3	Exponential	4.74		7.02	0.9642
	NDVI	Exponential	4.20		0.00118	0

Exponential model

$$\gamma(h) = c_0 + c\left\{1 - \exp\left(-\frac{h}{r}\right)\right\} \quad \text{for} \quad h > 0$$
$$\gamma(0) = 0$$

Spherical model

$$\gamma(h) = c_0 + c\left\{\frac{3}{2}\frac{h}{a} - \frac{1}{2}\left(\frac{h}{a}\right)^3\right\} \quad \text{for} \quad 0 < h \leq a$$
$$\gamma(h) = c_0 + c \quad \text{for} \quad h > a$$
$$\gamma(0) = 0$$

Pentaspherical model

$$\gamma(h) = c_0 + c\left\{\frac{15}{8}\frac{h}{a} - \frac{5}{4}\left(\frac{h}{a}\right)^3 + \frac{3}{8}\left(\frac{h}{a}\right)^5\right\} \quad \text{for} \quad 0 < h \leq a$$

$$\gamma(h) = c_0 + c \quad \text{for} \quad h > a$$

$$\gamma(0) = 0$$

The results of this analysis confirm that the scale of spatial variation identified in the SPOT image does correspond with changes on the ground. What we have done is to determine the scale and the structure of the variation quantitatively. In particular the scale of variation of the sum of the indicators of the ground cover is similar to the average short-range variation in the NDVI of the transect data. Evidently the image provides a good guide to approximate scales of spatial variation in ground cover, and this intuitive appreciation has been determined and described quantitatively.

Transect Survey: Results of Other Analyses

We analysed the information of the ground cover classes in conjunction with the image information along the ten transects. For this we had to isolate the waveband values for each transect from the full set of data to match the pixel information to the records of ground cover. This required new programming. The information was analysed by a one-way analysis of variance and correlation analysis. The results showed that channels 2 and 3 (red and infra-red) are strongly correlated with each other, but that channel 1 (green) is only weakly correlated with the others, Table 5. The ground cover classification accounted for only 6.49% of the variation in waveband 1, probably because in the fall all the conifers are much the same shade of green. Channels 2 and 3 accounted for 49.7% and 46.2% of the variation respectively.

Table 5. Correlation matrix of the three channels for the transect data

channel	1	2
2	0.1279	
3	0.0988	0.8984

Although channel 1 has the largest mean value and from the pixel map appears to be the most variable, channel 2 has the largest coefficient of variation of 15.6%

compared with 12% and 7.9% respectively for channels 1 and 3. These results suggest that, in this instance, channel 2 carries more information on variation in the vegetation than the others. An examination of the mean waveband values for channel 2 in relation to the ground cover showed that the differences between several classes is small. This raises the question as to how reliable a map based on a classification of the pixel values would be. This will be tested in due course.

In addition we did a canonical variate analysis to examine the degree of separation or overlap of the ground cover classes in all three channels simultaneously. Figure 11 shows the distribution of the sampling points plotted in the plane of the first two canonical variates, which account for 95% of the variance among classes, together with the centroids of the classes. The centroid of the military ground is quite separate from those of the other classes, which overlap one another considerably. This suggests that classification based on spectral information would be weak in discriminating between different kinds of vegetation cover. It also suggests that much of the success of the univariate analysis of variance arises from the differences between military ground and all other classes. This could be checked later.

We computed cross variograms between each type of ground cover and the three SPOT channels. Many of these fluctuated from positive increasing to decreasing to negative decreasing; others fluctuated in the opposite sense. Yet others are more erratic. We cannot explain this behaviour on scientific grounds. It seems possible that it is an artifact of the technology, and this should be investigated.

SECOND SAMPLING AND CONCLUSIONS

To map the variation in ground cover precisely by kriging, or indeeed any method of interpolation, would require different optimal sampling intervals for the different kinds of cover depending on the structure of their spatial variation. However, an average separation had to be determined practically, and we based it on the average range of all of the variograms. This was about 15 pixels (300 m). The absolute maximum separation to resolve the pattern is therefore 7.5 pixels (150 m), i.e. half of the correlation range. Classes occupying smaller patches than this would not be resolved, but those with larger ones would be. If the sampling interval were to approach 300 m then the data would contain no dependence. The only satisfactory way of mapping such data then would be by using point symbols.

This posed a problem because the effort needed to map the short-range variation in ground cover was neither available nor affordable. This is a general problem where there is much short-range variation and the methodological requirements conflict with what is feasible.

Essentially there are two approaches to designing a sampling scheme: one may either sample to optimize estimation by interpolation, by kriging for example, or classification, or choose the maximum affordable sample and distribute the sampling points to optimize estimation. In this case 100 sampling locations was the maximum

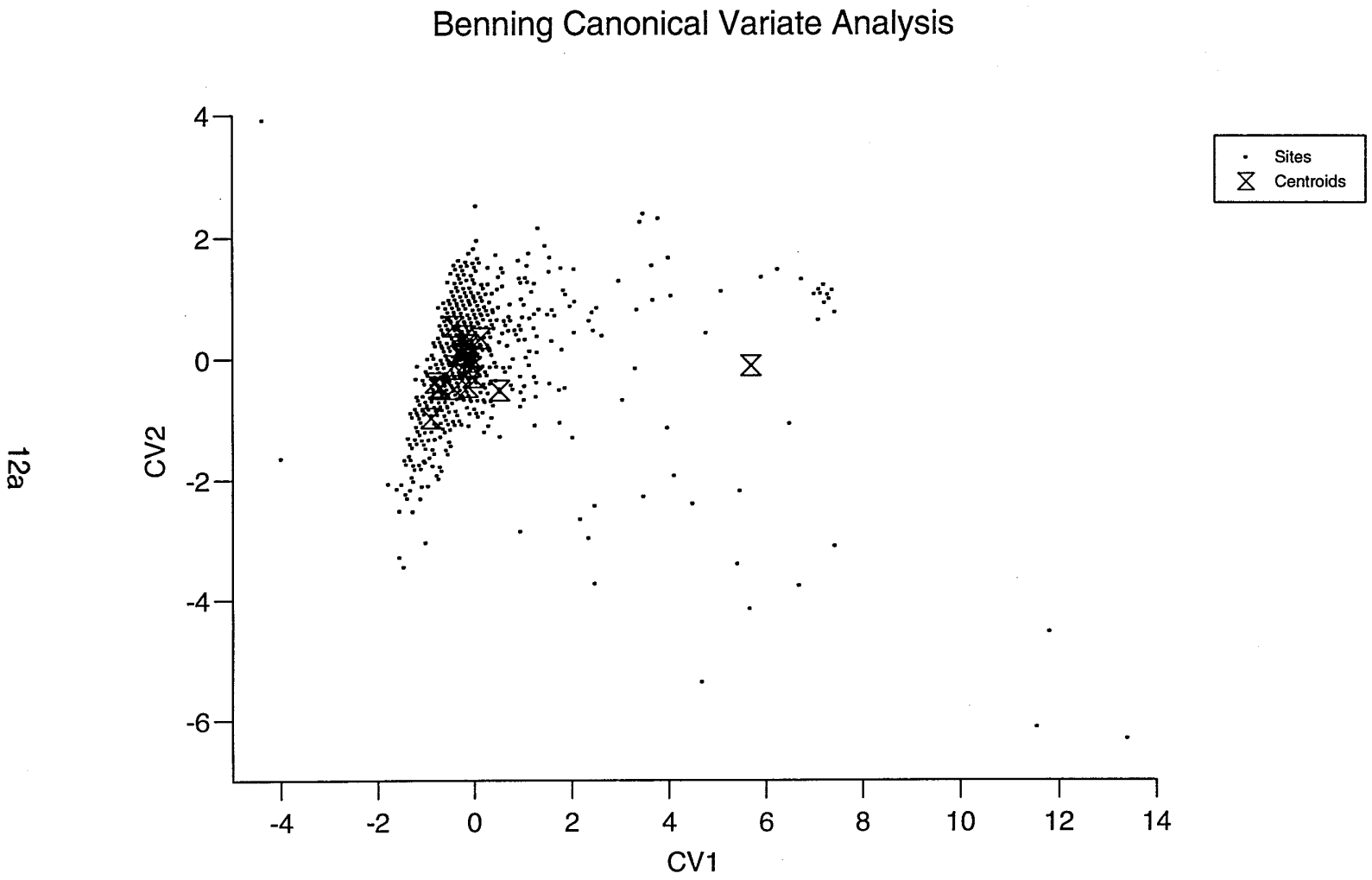

12a

Figure 11. Transect sites plotted in the plane of the first two canonical variates.

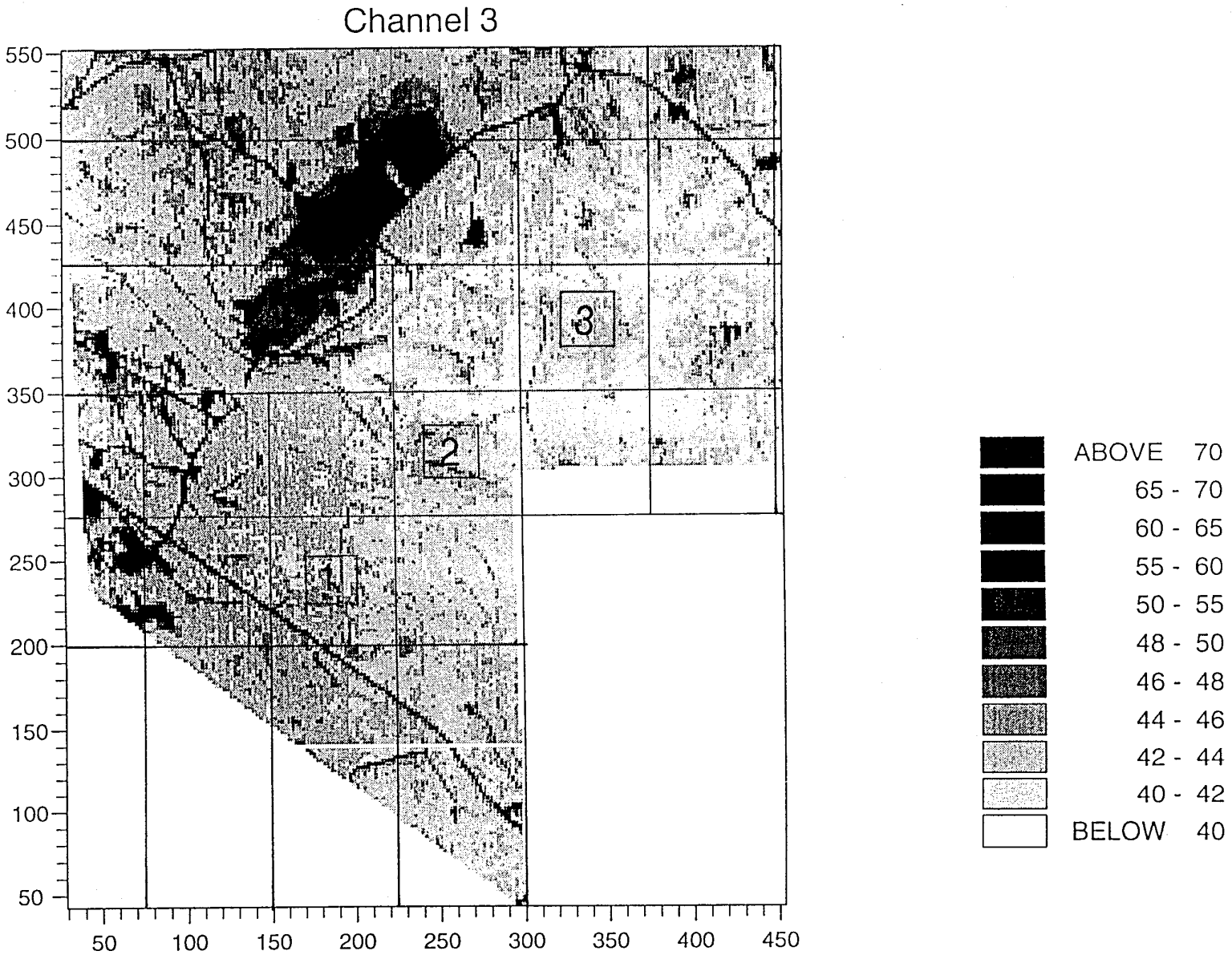

Figure 12. Map showing grid sampling in southern part of study area.

that could be achieved in the time available.

It is clear from both the analysis of the image and the ground cover that there is much short-range variation. The policy-makers and rangeland managers therefore have to decide whether they want or need this degree of resolution. The alternative would be to concentrate on the longer-range variation, of almost 3 km, which merely represents the major areas of different kinds of cover, such as forest and non-forest. To sample in an *ad hoc* manner at the intensity that can be afforded without regard to the spatial scale at which most of the variation occurs and to the kind of estimates required is likely to result in a waste of sampling effort. All methods of interpolation depend on spatially dependent data, whereas classification pixel by pixel does not.

The sampling scheme devised was a compromise to take into account the short-range variation, yet provide reasonable cover of just over half of the Region for mapping. A grid with a large interval of 1500 m (75 pixels), based on half the correlation range of the coarse pattern, was placed over the southern and eastern parts of the image, Figure 11. The vegetation classes of most interest were the long-leaf pine and the loblolly pine because it is in these that the rare red cockaded woodpecker lives, and based on the degree of variation in ground cover a fine resolution would be needed to map its potential habitat precisely. Based on the information from the ground cover transects three grid squares containing these types of cover were chosen for more detailed sampling. The coordinates of their top left hand corners are: (1) 170, 250; (2) 240, 330; and (3) 320, 410. A 150 m $\times$ 150 m grid with 25 sampling points at the nodes was nested within each of these larger squares (Figure 12). The advantage of this scheme was that both the broad and the detailed scales could be represented.

In the event the members of the team at TEC decided on a random sampling scheme that covered the entire Region with only 50 sample locations. The reason for adopting this approach was to attempt to compare the results of this investigation with the map produced conventionally. This sampling intensity can represent only the long-range variation. However, TEC believes that it could implement the scheme recommended, and it intends to apply this approach to sampling at the next stage of the work. The variogram analysis gace TEC two possible choices in this instance: to sample intensely to map the variation in detail or to sample sparsely and so pick up only the broad changes in ground cover. The spatial information enables an objective decision to be made about which procedure to adopt, i.e. detailed or sparse sampling, and to assess the reliability of the map resulting from the ground sampling.

At this stage our most important finding is that the pattern in the information in the wavebands reflects accurately the ground cover. So, one can decide how intensely to sample from analysing the SPOT imagery directly. The nested grid sampling scheme recommended for the second stage of field work seems the best way forward practically. TEC clearly did not have the resources to sample and map the whole Region in detail. Perhaps it need not in most of the Region, but in those critical parts of the Region where there are endangered species, it should devote effort for

detailed sampling and mapping. Essentially it should use a hierarchy of sampling effort that will be reflected in the accuracy of the maps.

BIBLIOGRAPHY

Atkinson, P. Curran, P. J. & Webster , R. (1990) Sampling remotely sensed imagery for storage, retrieval and reconstruction. *Professional Geographer*, **42**, 345-353.

Atkinson, P., Webster, R. & Curran, P. J. (1992). Cokriging with ground-based radiometry. *Remote Sensing of Environment*, **41**, 45-60.

Atkinson, P., Webster, R. & Curran, P. J. (1994). Cokriging with airborne MSS imagery. *Remote Sensing of Environment*,

Besag, J. (1986). On the statistical analysis of dirty pictures. *Journal of the Royal Statistical Society, Series B*, **48**, 559-502.

Bonifazi, G., Burrascano, P. & Volpi, F. (1993). A neural net based classification approach to discriminate between different urban areas. In: *Preprints of 3rd CODATA Conference, Enschede.*

Caillol, H., Hillion, A. L. & Pieczynski, W. (1993) Fuzzy random fields and unsupervised image segmentation. *IEEE Transactions on Geoscience and Remote Sensing*, **31**, 801-810.

Curran, P. J. *Principles of Remote Sensing*, Longmans, London.

Curran, P. J. The semi-variogram in remote sensing: An introduction. *Remote Sensing of Environment*, **28**, 493-507.

Goossens, M. A., Fabbri, A. G. & Gorte, B. G. H. (1993). Spatial filtering techniques in the classification of remotely sensed information. In: *Preprints of 3rd CODATA Conference, Enschede.*

Jupp, D. L. B., Strahler, A. H. & Woodcock, C. E. (1988). Autocorrelation and regularization in digital images. I. Basic theory. *IEEE Transactions on Geoscience and Remote Sensing*, **26**, 563-473.

Langford, M. (1993) *ERDAS Imagine Workbook*, Advisory Group on Computer Graphics.

Remote Sensing Society (1984). *Satellite Remote Sensing.* Proceedings of the Tenth International Conference, Reading.

Richards, J. A. (1993). *Remote Sensing Digital Image Analysis*, Springer-Verlag, Berlin.

Ross, G. J. S. (1987) *MLP User Manual*, Numerical Algorithms Group, Oxford.

Thomas, I. L., Benning, V. M. & Ching, N. P. (1987) *Classification of Remotely Sensed Images.* Adam Hilger, Bristol.

Van Der Meer, F. (1993). Classification of high spectral resolution imagery using an indicator kriging based technique. In: A. Soares (editor), *Geostatistics Tróia '92, Volume 2*, Kluwer Academic Publishers, pp. 829-840.

Vairinho, M. Pina, P. Sousa, A. J., Muge, F. & Oliveira, V. (1993) Geostatistics and image analysis in the interpretation of geochemical data. *CODATA Conference Preprints, Enschede, 1992.*

Webster, R., Curran, P. J. & Munden, J. W. (1989). Spatial correlation in reflected radiation from the ground and its implications for sampling and mapping by ground-based radiometry. *Remote Sensing of Environment*, **29**, 67-78.

Woodcock, C. E., Strahler, A. H. & Jupp, D. L. B. (1988 a). The use of variograms in remote sensing. I. Scene models and simulated images. *Remote Sensing of Environment*, **25**, 323-348.

Woodcock, C. E., Strahler, A. H. & Jupp, D. L. B. (1988 b). The use of variograms in remote sensing. II. Real digital images *Remote Sensing of Environment*, **25**, 349-379.